Condition monitoring of electro-mechanical actuators for aerospace using batch change detection algorithms

Mirko Mazzoleni, Matteo Scandella, Yamuna Maccarana, Fabio Previdi, Giulio Pispola, Nicola Porzi

Abstract— This paper proposes the use of a change detection algorithm to monitor the degradation of mechanical components of Electro-Mechanical Actuators (EMA) employed in the aerospace industry. Contrary to the standard on-line application of change detection methods, the presented approach can be applied in a batch mode, leveraging on the knowledge of when the data were collected. The methodology is applied to data measured during an endurance test campaign on a real EMA employed in aerospace, by means of a developed test bench, progressively bringing the EMA to failure. Three rationales for building an indicator of degradation are tested. Results show how the method is able to assess the degradation of the actuator over time, constituting a first step towards a condition monitoring solution for the more-electric-aircraft of the future.

I. INTRODUCTION

The envisioned future for the aerospace industry is towards the the More Electric Aircraft (MEA) initiative [1]. The aim is to replace the current hydraulic actuation [2] with an electro-mechanical one. This would lead to both environmental and efficiency benefits [3]. However, limited in-service experience of EMAs requires intensive research in order to show that they match the superior reliability levels of hydraulic systems. In order to pursue this objective, companies and universities are working together in synergy. One of the main topics where those subjects are focusing is the field of Condition Monitoring (CM) of Electro-Mechanical Actuators (EMA) [4].

These joint collaborations are often promoted and incentivized by the European Union (EU) or by the United States (US). As recent examples, authors in [5], [6], [7] provided several different solutions for fault detection of EMAs used in airliner applications, using a large experimental test campaign. The works were related to the FP7 EU-funded HOLMES (Health OnLine Monitoring for Electro-Mechanical actuator Safety) project. In the same way, the NASA funded several projects of fault detection in aerospace using a flyable test-bed [8], [9].

The present work is developed in the context of the H2020 EU-funded REPRISE (Reliable Electromechanical actuator for PRImary SurfacE with health monitoring) project [10]. The aim of the project is to support the improvement of the Technological Readiness Level (TRL) for a Flight-Control System (FCS) of small aircrafts, bringing it to TRL 5. A critical part of the work is the development of a condition monitoring strategy, able to provide a continuous assessment of the EMA health state, tracking the progressive faults degradation. In order to purse this goal, an extensive endurance experimental activity has been performed on a 1:1 scale EMA employed in aerospace. Experimental data have been measured in order to develop CM algorithms. The proposed monitoring algorithm leverages on the information acquired from the test bench, in order to assess the progressive degradation.

Condition monitoring approaches for EMAs already faced in the literature are, in addition to those aforementioned ones, presented in [11], [12], [13]. In the first work, the authors proposed a model-based approach tracking the estimates of a model's parameters. In the second work, the health monitoring strategy is based on EMAs' position-tracking performance. The last work employs a fault detection strategy based on vibration analysis.

The work presented in this paper differs from the previously cited ones, since it relies on an *unsupervised nonparametric data-driven* method, *using only* features computed from phase-current measurements. The method employed here is a change-detection algorithm based on *density-ratio estimation* [14]. The rationale of the method consists into assessing if a change occurred between the probability distributions of data samples over past and present intervals. The assumption is to relate the motor degradation to a distributional change in its measured data.

Change-point detection methods are usually classified into real-time [15] and retrospective detection [16]. The difference lies in the immediate response of the former methodologies, with respect to the greater accuracy and higher computation times of the latter ones. Other change detection methods relies instead on ideas from subspace methods, usually employed in system identification [17].

In its basic form, the algorithm employed in this paper belongs to the retrospective category. However, we propose to use the method in a *batch* manner, with respect to the *on-line* fashion. This is possible by planning regular checks of the mechanical component, and comparing the previously measurements with the currently performed ones. If the system detects that the data distribution is changed between the two *known* time instants, than we can suspect a degradation of the EMA functionalities in the meantime. By comparing measured data with a "gold standard" set of measures (for example a healthy dataset at the beginning of actuator's life), it would be also possible to detect small changes that, with the standard on-line methods, would be more difficult to recognize. A first version of this algorithm

G. Pispola and N.Porzi are with the company UMBRAGROUP spa, 06034 Foligno (PG), Italy. M. Mazzoleni, M. Scandella, Y. Maccarana and F. Previdi are with the Department of Management, Information and Production Engineering, University of Bergamo, Via G. Marconi 5, 24044 Dalmine (BG), Italy. Email to: mirko.mazzoleni@unibg.it.

that works in an on-line manner has been presented in [18].

The remainder of the paper is organized as follows. Section II presents the experimental setup deployed for the performed endurance tests on the EMA. Section III formulates the change-detection problem. In Section IV, the density-ratio change detection method is adapted to perform the batch condition monitoring of the EMA under study, discussing also experimental results on data measured from an endurance test campaign. Lastly, Section VI is devoted to concluding remarks and future developments.

II. Experimental Setup

A test bench is employed to perform the endurance tests on the EMA, see Figure 1. The EMA is a three-phases brushless DC motor, capable to operate even in case of one supply loss. A LVDT sensor is used for the position control loop. A ballscrew transmission, with 8 circuits with 1 turn each transforms the rotational motion in the linear one. The three phase currents are measured by means of LEM sensors. A linear motor provides the simulated load.
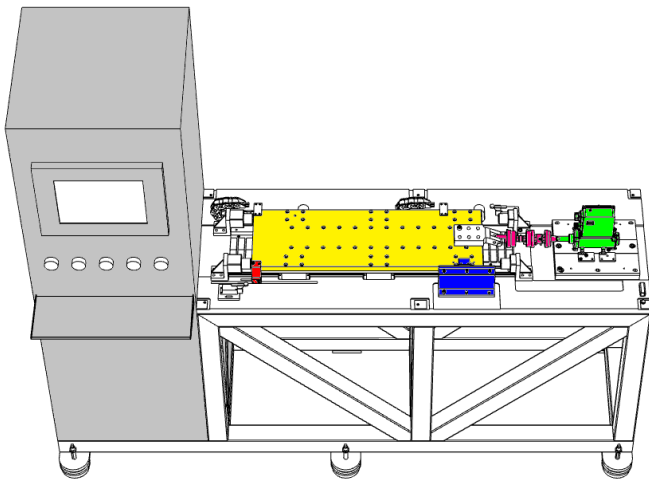

Fig. 1. Schematic of the test bench. (Yellow)) linear motor, (Green) EMA, (Pink) load cell, (Blue) absolute linear optical encoder.

Reference position profiles employed during the test were sinusoidal. The rationale for this choice is that, during operation, the EMA has to actuate forward and backward the main flight control surfaces. The bandwidth of the position control loop is about 1.5Hz. The used sinusoids' amplitudes ranged from 5mm to 30mm. The used sinusoids' frequencies ranged from 0.1Hz to 10Hz. In order to accelerate the degradation process of EMA, 3 out of 8 balls circuits were used. This increased the pressure at the contact points between the balls and the screw thread. Then, the EMA undergone heavier conditions than standard operating ones. Furthermore, the EMA has been connected to the linear motor so that the 17% of the axial load force will generate also a radial component. The chosen load conditions are: i) *H0 (nominal) condition*, 300N of constant load; ii) *H1 (overload) condition*, 800N of constant load; iii) *H1b (overload) condition*, 1200 of constant load. These loads were chosen after a Finite Element Method (FEM) analysis,

that showed the pressures undergone by the steel balls inside the ballscrew. The overload conditions correspond to loads where the balls are over-stressed. The EMA suffered fatigue tests at conditions H1 and H1b. Measurements for the condition assessment were taken after every endurance sessions, in the H0 condition. Three different testing regimes were envisaged, with a different degree of lubrication. The *Normal lubrication* regime consisted in the nominal operating condition, that is, with the lubricant normally employed in this type of mechanical transmissions. The *Poor lubrication* regime was characterized by *partially* removing the lubricant. The *No lubrication* regime *completely* removed the lubricant. These choices were motivated by considering that the loss of lubricant could be a possible scenario, leading to malfunctioning of the EMA.

Figure 2 reports the performed tests since April 2017, showing both the number of revolutions done by the ballscrew, and the distance that it traveled performing the tests. The motor performed 2.582.933 ca. revolutions in
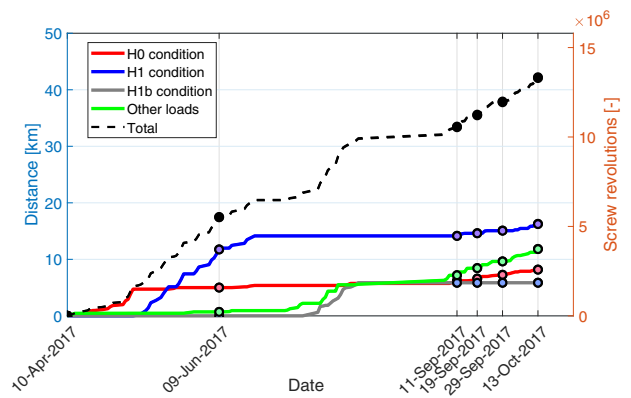

Fig. 2. Performed test conditions with number of revolutions and distance performed during six months.

H0 condition; 5.130.369 ca. in H1 condition; 1.850.274 ca. in H1b condition; 3.732.531 ca. in other loads conditions. These are referred to tests performed at different loads, for examples to compute the bode diagram (under no load) or tests related to assess the bench functionalities. In total, the EMA performed 13.296.113 revolutions. When reporting these numbers, we discarded decimals of revolutions. These numbers were computed by carefully considering the dynamic response of the system. This was possible after an estimation of the Bode diagram of the system, via a sinusoidal input sweep. As additional information, the motor traveled 42,215km ca.

III. Change detection via relative density-ratio estimation

A. Problem statement

The proposed algorithm is a density-ratio estimation method known as *Relative unconstrained Least-Squares Importance Fitting* (RuLSIF) [19], [14]. The assumption is that the estimation of the *ratio* of two densities is
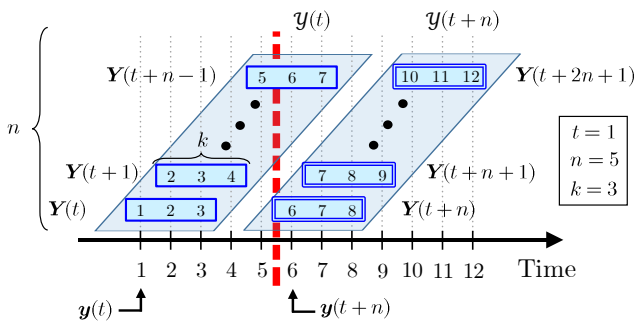
Fig. 3. Schematic representation of the notation for a one-dimensional time series, for illustrative settings such that $d = 1, t = 1, n = 5$ and $k = 3$.

substantially easier than estimating the two densities in a separate way [20]. In our setting, the two densities represents kernel estimates of the time series data distribution, before and after a certain time instant. Then, using a suitable divergence, it is possible to estimate how the two densities differ. Let $\boldsymbol{y}(t) \in \mathbb{R}^{d \times 1}$ be a d-dimensional time-series sample at time t. Let's define

$$\boldsymbol{Y}(t) \equiv \left[\boldsymbol{y}(t)^{\mathrm{T}}, \, \boldsymbol{y}(t+1)^{\mathrm{T}}, \, \cdots, \, \boldsymbol{y}(t+k-1)^{\mathrm{T}}\right]^{\mathrm{T}} \in \mathbb{R}^{d \cdot k \times 1}$$

as a "subsequence" [1] of time-series of length k, at time t. The subsequence $\boldsymbol{Y}(t)$ is treated as a single data sample. We then define the quantity $\mathcal{Y}(t)$ as the matrix composed by n of the dk-th dimensional samples $\boldsymbol{Y}(t)$, starting from t:

$$\mathcal{Y}(t) \equiv [\boldsymbol{Y}(t), \, \boldsymbol{Y}(t+1), \, \cdots, \, \boldsymbol{Y}(t+n-1)] \in \mathbb{R}^{d \cdot k \times n}.$$

The matrix $\mathcal{Y}(t)$ forms a *Hankel matrix*, playing a key role in change-point detection based on subspace learning [17]. Consider now two consecutive segments $\mathcal{Y}(t)$ and $\mathcal{Y}(t+n)$. The change-detection problem is then solved by computing a certain dissimilarity measure between $\mathcal{Y}(t)$ and $\mathcal{Y}(t+n)$. The higher the dissimilarity measure is, the more likely the two distributions differ. The entire notations are depicted schematically in Figure 3.

B. Divergence measures

Denote now the probability distributions of the samples in $\mathcal{Y}(t)$ and $\mathcal{Y}(t+n)$ as P and P', respectively. The Pearson divergence is defined as [21]:

$$\mathrm{PE}\left(P \,\|\, P'\right) \equiv \frac{1}{2} \int p'(\mathbf{X}) \cdot \left(\frac{p(\mathbf{X})}{p'(\mathbf{X})} - 1\right)^2 d\mathbf{X}, \quad (1)$$

where $\mathbf{X}$ denotes the generic dk-th dimensional random variable, and $p(\mathbf{X})$, $p'(\mathbf{X})$ are the probability density functions of P and P', respectively.

Let now $\{\mathbf{Y}_i\}_{i=1}^n$ and $\{\mathbf{Y}'_j\}_{j=1}^n$ be a set of samples drawn from $p(\mathbf{X})$ and $p'(\mathbf{X})$. In order to compute (1), we will employ an *estimate* of the density-ratio $\frac{p(\mathbf{X})}{p'(\mathbf{X})}$, using proper sets of samples which are representative of the two distributions. The samples $\{\mathbf{Y}_i\}_{i=1}^n$ are those belonging to

$\mathcal{Y}(t)$. The samples $\{\mathbf{Y}'_j\}_{j=1}^n$ are those belonging to $\mathcal{Y}(t+n)$. The density-ratio value $\frac{p(\mathbf{X})}{p'(\mathbf{X})}$ in (1) could be unbounded, depending on the condition of the denominator density $p'(\mathbf{X})$. To overcome this problem, the α-relative Pearson divergence measure was introduced in [14], for $0 \leq \alpha < 1$:

$$\mathrm{PE}_\alpha \left(P \,\|\, P'\right) \equiv PE \left(P \,\|\, \alpha P + (1-\alpha) P'\right)$$
$$= \frac{1}{2} \int p'_\alpha(\mathbf{X}) \cdot \left(\frac{p(\mathbf{X})}{p'_\alpha(\mathbf{X})} - 1\right)^2 d\mathbf{X}, \quad (2)$$

where $p'_\alpha(\mathbf{X}) = \alpha p(\mathbf{X}) + (1-\alpha) p'(\mathbf{X})$ is the α-*mixture density*. The α-*relative density-ratio* is then defined as:

$$r_\alpha(\mathbf{X}) = \frac{p(\mathbf{X})}{p'_\alpha(\mathbf{X})} = \frac{p(\mathbf{X})}{\alpha p(\mathbf{X}) + (1-\alpha) p'(\mathbf{X})}, \quad (3)$$

which reduces to plain density-ratio when $\alpha = 0$, and it is bounded above by $1/\alpha$ for $\alpha > 0$, even when the plain density-ratio $\frac{p(\mathbf{X})}{p'(\mathbf{X})}$ is unbounded.

It is important to notice that neither (1) nor (2) are metrics, since they are not symmetric and the triangular inequality does not hold. To cope with the first problem, authors in [14] proposed to use the symmetrical divergence:

$$\mathrm{PE}_\alpha \left(P \,\|\, P'\right) + \mathrm{PE}_\alpha \left(P' \,\|\, P\right), \quad (4)$$

where each term is estimated separately. However, divergence (4) still not satisfies the triangle inequality.

C. Learning algorithm

The α-*relative density-ratio* is modeled as:

$$g\left(\mathbf{X}; \boldsymbol{\theta}\right) \equiv \sum_{l=1}^n \theta_l \cdot K\left(\mathbf{X}, \mathbf{Y}_l\right), \quad (5)$$

where $\boldsymbol{\theta} = [\theta_1, \ldots, \theta_n]^{\mathrm{T}} \in \mathbb{R}^{n \times 1}$ are unknown parameters, $K\left(\cdot, \cdot\right)$ is a kernel basis function, and $\mathbf{Y}_l$ refers to the l-th data sample in $\mathcal{Y}(t)$. In our experiments, we employ the Gaussian kernel such that:

$$K\left(\mathbf{Y}_1, \mathbf{Y}_2\right) = \exp\left(-\frac{\|\mathbf{Y}_1 - \mathbf{Y}_2\|^2}{2\delta^2}\right), \quad (6)$$

where $\delta > 0$ is the kernel width. The parameters' vector $\boldsymbol{\theta}$ is learned by minimizing the squared loss:

$$J(\boldsymbol{\theta}) = \frac{1}{2} \int p'_\alpha(\mathbf{X}) \left(r_\alpha(\mathbf{X}) - g(\mathbf{X}; \boldsymbol{\theta})\right)^2 d\mathbf{X}$$
$$= \frac{1}{2} \int p'_\alpha(\mathbf{X}) r_\alpha^2(\mathbf{X}) \, d\mathbf{X} - \int p(\mathbf{X}) g(\mathbf{X}; \boldsymbol{\theta}) \, d\mathbf{X}$$
$$+ \frac{\alpha}{2} \int p(\mathbf{X}) g(\mathbf{X}; \boldsymbol{\theta})^2 \, d\mathbf{X} + \frac{1-\alpha}{2} \int p'(\mathbf{X}) g(\mathbf{X}; \boldsymbol{\theta})^2 \, d\mathbf{X}$$
$$(7)$$

where the computations were made by expanding the square and employing the definition of $p'_\alpha(\mathbf{X})$.

The first term of (7) can be discarded since it does not depend on the unknown parameters. By substituting $g(\mathbf{X}; \boldsymbol{\theta})$ with the definition (5), and approximating the expectations with empirical averages, it is possible to obtain the following minimization problem (with the addition of the

Ridge regularization term $\frac{\lambda}{2}\boldsymbol{\theta}^{\mathrm{T}}\boldsymbol{\theta}$):

$$\widehat{\boldsymbol{\theta}} = \arg\min_{\boldsymbol{\theta}\in\mathbb{R}^n} \left[\frac{1}{2}\boldsymbol{\theta}^{\mathrm{T}}\widehat{\boldsymbol{H}}\boldsymbol{\theta} - \widehat{\boldsymbol{h}}^{\mathrm{T}}\boldsymbol{\theta} + \frac{\lambda}{2}\boldsymbol{\theta}^{\mathrm{T}}\boldsymbol{\theta}\right], \quad (8)$$

where $\widehat{\boldsymbol{H}} \in \mathbb{R}^{n\times n}$, $\widehat{\boldsymbol{h}} \in \mathbb{R}^{n\times 1}$ and $\lambda > 0$ controls the regularization strength. The element in position (l,m) of $\widehat{\boldsymbol{H}}$ is given by:

$$\widehat{H}_{(l,m)} = \frac{\alpha}{n}\sum_{i=1}^{n} K(\mathbf{Y}_i, \mathbf{Y}_l) \cdot K(\mathbf{Y}_l, \mathbf{Y}_m)$$
$$+ \frac{1-\alpha}{n}\sum_{j=1}^{n} K(\mathbf{Y}'_j, \mathbf{Y}_l) \cdot K(\mathbf{Y}'_j, \mathbf{Y}_m). \quad (9)$$

The element in position l of $\widehat{\boldsymbol{h}}$ is given by:

$$\widehat{h}_{(l)} = \frac{1}{n}\sum_{i=1}^{n} K(\mathbf{Y}_i, \mathbf{Y}_l). \quad (10)$$

The solution to problem (8) can expressed as:

$$\widehat{\boldsymbol{\theta}} = \left(\widehat{\mathbf{H}} + \lambda\boldsymbol{I}_n\right)^{-1} \cdot \widehat{\boldsymbol{h}}, \quad (11)$$

where $\boldsymbol{I}_n$ is n-th dimensional identity matrix. The density ratio estimator assumes thus the form of:

$$\widehat{g}(\mathbf{X}) = \sum_{l=1}^{n} \widehat{\theta}_l \cdot K(\mathbf{X}, \mathbf{Y}_l). \quad (12)$$

D. Computing the divergence

In order to use (12), it is first necessary to rewrite the Pearson divergence (2) as:

$$\begin{aligned}\mathrm{PE}_\alpha\left(P\,\|\,P'\right) &= \tfrac{1}{2}\int p'_\alpha(\mathbf{X}) \cdot \left(\frac{p(\mathbf{X})}{p'_\alpha(\mathbf{X})} - 1\right)^2 d\mathbf{X}\\ &= \frac{1}{2}\int p'_\alpha(\mathbf{X}) \cdot \left(\frac{p(\mathbf{X})^2}{p'_\alpha(\mathbf{X})^2} - 2\frac{p(\mathbf{X})}{p'_\alpha(\mathbf{X})} + 1\right) d\mathbf{X}\\ &= \frac{1}{2}\int \left(\frac{p(\mathbf{X})^2}{p'_\alpha(\mathbf{X})} - 2p(\mathbf{X}) + p'_\alpha(\mathbf{X})\right) d\mathbf{X}\\ &= \frac{1}{2}\int \left(\frac{p(\mathbf{X})}{p'_\alpha(\mathbf{X})}\right) \cdot p(\mathbf{X})\, d\mathbf{X} - \frac{1}{2},\end{aligned} \quad (13)$$

where the simplification in the last step follows since probability distributions integrate to one. Substituting the estimator (12) in (13), and approximating the integrals with empirical averages, leads to the following approximation of the α-relative divergence:

$$\widehat{\mathrm{PE}}_\alpha = \frac{1}{2n}\sum_{i=1}^{n} \widehat{g}(\mathbf{Y}_i) - \frac{1}{2}. \quad (14)$$

The final computed score is then, as reported by (4), the quantity $\Pi \equiv \widehat{\mathrm{PE}}_\alpha(P\,\|\,P') + \widehat{\mathrm{PE}}_\alpha(P'\,\|\,P)$.

IV. CONDITION MONITORING

A. Feature extraction

The aim of this work is to not use standard vibration measurements to detect mechanical faults. Instead, we relied

only on currents signals. The inputs for the change detection algorithm are, therefore, features computed from phase current measurements. The rationale is that a degraded motor will drain more current to perform the same operations. Notice that, since the EMA is closed-loop controlled, until the power supply can provide enough energy, *we do not see any degradation* in position tracking. Monitoring the control actions, in this case the phase currents, helps into identifying possible causes of malfunction.

Consider now the three phase currents, $i_a(t), i_b(t), i_c(t)$, measured during an experiment. Since the measured position is a sinusoid with period $T = 2\pi/\omega$, with ω the frequency measured in rad/s, it is possible to write the current signal of the x-th phase as:

$$i_x(t), \quad (\tau - 1) \cdot T \le t \le \tau \cdot T, \quad (15)$$

with $x = a, b, c$ and $\tau = 1, \ldots, N_p$, being N_p the total number of periods in the considered experiment. For each period, various indicators are computed. If the change detection algorithm detects that the *sampling distribution of the indicators* is changed, this is a symptom that the system degraded its functioning. We computed the Root Mean Square (RMS) value and the Crest Factor (CF) from currents signals. The RMS is computed for each phase current $x = a, b, c$ *over a single period* $\tau = 1, \ldots, N_p$ as:

$$\sigma_x(\tau) = \sqrt{\frac{1}{T} \cdot \sum_{t=(\tau-1)\cdot T}^{\tau\cdot T} i_x^2(t)}. \quad (16)$$

For each experiment, it is possible compute a mean RMS value at every period $\tau = 1, \ldots, N_p$ as:

$$\Sigma(\tau) = \frac{1}{3} \cdot \left(\sigma_a(\tau) + \sigma_b(\tau) + \sigma_c(\tau)\right) \in \mathbb{R} \quad (17)$$

The CF index is computed, for $(\tau - 1) \cdot T \le t \le \tau \cdot T$ as:

$$\gamma_x(\tau) = \frac{\max\left(|i_x(t)|\right)}{\sigma_x(\tau)}. \quad (18)$$

For each experiment, it is possible compute a mean CF value at every period $\tau = 1, \ldots, N_p$ as:

$$\Gamma(\tau) = \frac{1}{3} \cdot \left(\gamma_a(\tau) + \gamma_b(\tau) + \gamma_c(\tau)\right) \in \mathbb{R} \quad (19)$$

A variation of the algorithm described in Section IV-B is applied to the features $\Sigma(\tau)$ and $\Gamma(\tau)$. These features have been computed for operating frequencies of 0.1Hz, 0.3Hz, 0.5Hz, 0.8Hz, 0.9Hz and 1Hz. These range of frequencies is those for which the EMA has been designed. In the present work, we reported the application of the change-detection method to the chosen frequency of 1Hz.

B. Batch change detection for EMA

As stated in the Section I, we applied the change detection algorithm of Section III in a *batch* fashion, instead of an *on-line* one. Thus, the algorithm compares the features computed on the new experiment with past ones. The rationale of applying a batch procedure is mainly due to the certainty that external conditions at which the experiments

are made can be set to remain the same every time this procedure is carried on. As an example, it is difficult to reliably estimate the load when the EMA operates in flight. Variations in load conditions can alter the decision of an on-line condition monitoring algorithm, that was designed to work on controlled test conditions. Another factor of variation can be the temperature, that can reach very low values at high altitudes. Obviously, the method requires a policy to chose the "reference measures" to be compared with the new acquired ones. In the following, three different rationales are compared, that is:

- **Always Healthy (AH)**: always compare with the healthy dataset
- **Always Previous (AP)**: always compare with the most recent dataset
- **Last Change (LC)**: always compare to the last dataset that triggered a predetermined threshold. The method generates a score, defined as the number of threshold violations.

For the application of the proposed methodology, we consider a total of $Q = 11$ experiments, performed at 1Hz with 10mm of position amplitude, in the H0 condition. The first two of these tests can be considered as *healthy state* experiments. Tests 3 and 4 have been performed after endurance sessions with *poor lubricant*. The remaining tests have been performed after endurace sessions with *no lubricant* at all. Contrary to the standard method of Section III, the proposed approach applies the algorithm *not* with a sliding window, but *directly* comparing measures acquired during one date to measurements acquired on a different date. The batch version of the method is represented in Figure 4.
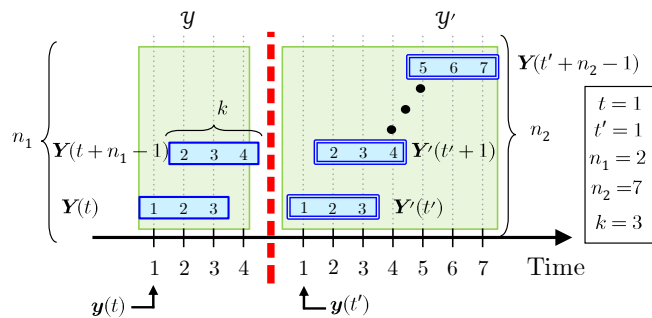

Fig. 4. Condition assessment via the batch RuLSIF method, with a one-dimensional time series, $d = 1$, and $k = 3$, $n_1 = 2$ and $n_2 = 7$.

Here there is not a continuous progression of the time series, since now the data are considered in a separate way, and not as a continuous stream of information. Thus, even the time indexes t and t' are different. The parameter k maintain its previous role. We denote with $\mathcal{Y}$ the first dataset, and with $\mathcal{Y}'$ the second one. Notice how $\mathcal{Y}$ and $\mathcal{Y}'$ do not depend on the time anymore. The number of observations in the two datasets, that depend on k, can be different. We denote with n_1 the number of observations in $\mathcal{Y}$, and with n_2 the number of observations in $\mathcal{Y}'$. Apart from these

considerations, the method computes the divergence between $\mathcal{Y}$ and $\mathcal{Y}'$ as previously described.

The considered time series has dimensionality $d = 2$. Each sample $\boldsymbol{y}(\tau) \in \mathbb{R}^{2 \times 1}$ is a vector which elements are $\Sigma(\tau)$ and $\Gamma(\tau)$. The same reasoning can be done with the data from $\mathcal{Y}'$. The parameter k plays the role of a "memory" which usually appears in dynamic systems. Since we computed the value of the considered time series as independent indicators at each period τ, we choose to set $k = 1$. Thus, we have that:

$$\boldsymbol{Y}(t) = \boldsymbol{y}(t) \in \mathbb{R}^{2 \cdot 1 \times 1}; \qquad \boldsymbol{Y}'(t') = \boldsymbol{y}'(t') \in \mathbb{R}^{2 \cdot 1 \times 1}. \quad (20)$$

The hyperparameters δ and λ are chosen via κ-fold cross-validation. Since we follow the heuristic rule to have at least $10 \cdot m$ data points, where m is the number of parameters to tune, it follows that we need at least 20 samples per fold. For this reason, we chose $\kappa = 5$. The heuristic condition was always met for all the datasets that we compared. We then adhered to the default value $\alpha = 0.5$ as in [14].

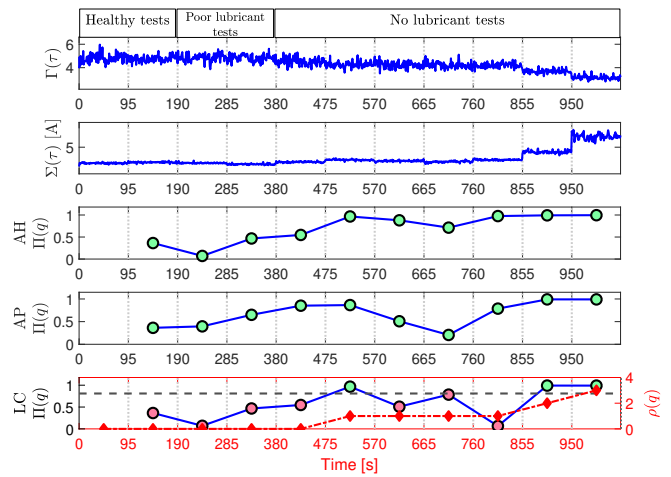Figure 5 show the results of applying the batch change detection algorithm to the three different policies.

Fig. 5. Condition assessment via the different batch strategies. The last plot depicts also the threshold η (dashed gray line) and the degradation score $\rho(q)$ (dotted red line). Vertical light gray bars represent the different experiments.

V. DISCUSSION OF THE RESULTS

The first two plots represent the computed values of RMS and CF. Light gray vertical lines separate one experiment from another. Each experiment is performed in a different date and in the same (nominal) load condition of 300N, after sessions of poor lubricant or no lubricant fatigue tests. Then, the scores $\Pi(q)$ of the change detection algorithm were computed for each dataset's comparison q. Since we have $Q = 11$ experiments, if follows that $q = 2, \ldots, Q$. In the "Always Healthy (AH)" policy, all tests from $q = 2$ are compared with the first healthy test. The AH strategy detects an increasing deviation over time from the healthy dataset, given by the increasing value of the score $\Pi(q)$. The drawback is that this policy does not give a degradation

index. In fact, if the EMA remains damaged with the same severity for multiple tests, the AH policy tells that there are changes with respect to the healthy test, but this is not an information about how much the EMA is degrading its functionalities. The policy "Always Previous (AP)" compares each dataset with the previous one. While solving the problem of the AH strategy, this rationale is not sensitive to slow changes in the EMA degradation. In fact, always comparing to the previous experiment in time can lead to little deviation from the previous data, and so the score will be low as well. To solve this, we propose the "Last Change (LC)" strategy. By comparing each new experiment with the last one that gave a significant value of the score $\Pi(q)$, we are able to assess even slow degradations. To define what significant means, we chose to set a threshold η at two times the value of the first score $\Pi(2)$. This is the detected difference from two consecutive healthy datasets. Notice how this threshold can be refined in various ways, such averaging more scores from different healthy sets. It is then possible to define a "degradation counter" $\rho(q)$, which tells how many tests of the LC policy are greater than the threshold η. This counter is represented in the last plot of Figure 5, and it is coherent with the motor degradation shown by the phase currents' indicators.

VI. Conclusions and future developments

This paper introduced the application of the change detection algorithm RuLSIF to perform condition monitoring of an electro-mechanical actuator, employed in aerospace environment. The RuLSIF method, usually employed in an on-line fashion, has been here used in a batch mode. The reason for this choice was to guarantee, up to a certain extent, that the conditions with which the experiments are carried out are the same. This will ensure that the condition monitoring application is able to detect changes due to a degradation of the EMA and not due to external factors. We then proposed three different policies of how this method should the interpreted to perform condition assessment. Out of the three, we found that the best strategy is that which compares a new dataset to the last one which gave a significant difference of the data distributions. Therefore, we built a simple degradation index to assess the overall EMA health state. Future research is devoted to perform a new test campaign with a new EMA of the same type, and testing the proposed method more extensively.

Acknowledgment

References

[1] A. Isturiz, J. Vinals, S. Fernandez, R. Basagoiti, E. d. l. Torre Arnanz, and J. Novo, "Development of an aeronautical electromechanical actuator with real time health monitoring capability," 2010.

[2] A. L. Cologni, M. Mazzoleni, and F. Previdi, "Modeling and identification of an electro-hydraulic actuator," in *Control and Automation (ICCA), 2016 12th IEEE International Conference on.* IEEE, 2016, pp. 335–340.

[3] G. Buticchi, L. Costa, and M. Liserre, "Improving system efficiency for the more electric aircraft: A look at dc\/dc converters for the avionic onboard dc microgrid," *IEEE Industrial Electronics Magazine*, vol. 11, no. 3, pp. 26–36, 2017.

[4] A. Garcia, I. Cusido, J. Rosero, J. Ortega, and L. Romeral, "Reliable electro-mechanical actuators in aircraft," *IEEE Aerospace and Electronic Systems Magazine*, vol. 23, no. 8, 2008.

[5] M. Mazzoleni, Y. Maccarana, and F. Previdi, "A comparison of data-driven fault detection methods with application to aerospace electro-mechanical actuators," *IFAC-PapersOnLine*, vol. 50, no. 1, pp. 12 797–12 802, 2017, 20th IFAC World Congress.

[6] M. Mazzoleni, G. Maroni, Y. Maccarana, S. Formentin, and F. Previdi, "Fault detection in airliner electro-mechanical actuators via hybrid particle filtering," *IFAC-PapersOnLine*, vol. 50, no. 1, pp. 2860 – 2865, 2017, 20th IFAC World Congress.

[7] M. Mazzoleni, S. Formentin, F. Previdi, and S. M. Savaresi, "Fault detection via modified principal direction divisive partitioning and application to aerospace electro-mechanical actuators," in *Decision and Control (CDC), 2014 IEEE 53rd Annual Conference on.* IEEE, 2014, pp. 5770–5775.

[8] E. Balaban, A. Saxena, S. Narasimhan, I. Roychoudhury, M. Koopmans, C. Ott, and K. Goebel, "Prognostic health-management system development for electromechanical actuators," *Journal of Aerospace Information Systems*, 2015.

[9] M. A. Ismail, "Vibration-based fault detection and quantification for primary flight control electro-mechanical actuators," in *Annual Conference of the Prognostics and Health Management Society.* PHM Society, 2017.

[10] M. Mazzoleni, Y. Maccarana, F. Previdi, G. Pispola, M. Nardi, F. Perni, and S. Toro, "Development of a reliable electro-mechanical actuator for primary control surfaces in small aircrafts," in *Advanced Intelligent Mechatronics (AIM), 2017 IEEE International Conference on.* IEEE, 2017, pp. 1142–1147.

[11] R. Dixon and A. Pike, "Application of condition monitoring to an electromechanical actuator: a parameter estimation based approach," *Computing & Control Engineering Journal*, vol. 13, no. 2, pp. 71–81, 2002.

[12] G. Di Rito, F. Schettini, and R. Galatolo, "Model-based health-monitoring of an electro-mechanical actuator for unmanned aerial system flight controls," in *Metrology for AeroSpace (MetroAeroSpace), 2017 IEEE International Workshop on.* IEEE, 2017, pp. 502–511.

[13] M. A. Ismail, E. Balaban, and H. Spangenberg, "Fault detection and classification for flight control electromechanical actuators," in *Aerospace Conference, 2016 IEEE.* IEEE, 2016, pp. 1–10.

[14] S. Liu, M. Yamada, N. Collier, and M. Sugiyama, "Change-point detection in time-series data by relative density-ratio estimation," *Neural Networks*, vol. 43, pp. 72–83, 2013.

[15] R. Garnett, M. A. Osborne, and S. J. Roberts, "Sequential bayesian prediction in the presence of changepoints," in *Proceedings of the 26th Annual International Conference on Machine Learning.* ACM, 2009, pp. 345–352.

[16] K. Yamanishi and J.-i. Takeuchi, "A unifying framework for detecting outliers and change points from non-stationary time series data," in *Proceedings of the eighth ACM SIGKDD international conference on Knowledge discovery and data mining.* ACM, 2002, pp. 676–681.

[17] Y. Kawahara, T. Yairi, and K. Machida, "Change-point detection in time-series data based on subspace identification," in *Data Mining, 2007. ICDM 2007. Seventh IEEE International Conference on.* IEEE, 2007, pp. 559–564.

[18] M. Mazzoleni, M. Scandella, Y. Maccarana, F. Previdi, G. Pispola, and N. Porzi, "Condition assessment of electro-mechanical actuators for aerospace using relative density-ratio estimation," 2018, 18th IFAC Symposium on System Identification SYSID 2018.

[19] T. Kanamori, S. Hido, and M. Sugiyama, "A least-squares approach to direct importance estimation," *Journal of Machine Learning Research*, vol. 10, no. Jul, pp. 1391–1445, 2009.

[20] M. Sugiyama, T. Suzuki, and T. Kanamori, *Density ratio estimation in machine learning.* Cambridge University Press, 2012.

[21] K. Pearson, "On the criterion that a given system of deviations from the probable in the case of a correlated system of variables is such that it can be reasonably supposed to have arisen from random sampling," in *Breakthroughs in Statistics.* Springer, 1992, pp. 11–28.